Applied Surface Science 393 (2017) 30–36

Contents lists available at ScienceDirect

Applied Surface Science

journal homepage: www.elsevier.com/locate/apsusc

Full length article

# Synthesis and characterization of advanced $Li_3V_2(PO_4)_3$ nanocrystals@conducting polymer PEDOT for high energy lithium-ion batteries

Haiyan Yan*, Gai Zhang, Yongfei Li

*School of Materials and Chemical Engineering, Xi'an Technological University, Xi'an 710021, PR China*

ARTICLE INFO

*Article history:*
Received 28 June 2016
Received in revised form
13 September 2016
Accepted 30 September 2016
Available online 1 October 2016

*Keywords:*
$Li_3V_2(PO_4)_3$ cathode
Conducting polymer
PEDOT
Lithium-ion batteries
Electrochemical performance

ABSTRACT

Monoclinic $Li_3V_2(PO_4)_3$ compound is gathering significant interest as cathode material for lithium-ion batteries at the moment because of its high theoretical capacity, good safety and low cost. However, it suffers from bad rate capability and short cycling performance duo to the intrinsic low electronic conductivity. Herein, we report a design of $Li_3V_2(PO_4)_3$ particles coated by conducting polymer PEDOT through a facile method. When the cell is tested between 3.0 and 4.3 V, the core-shell $Li_3V_2(PO_4)_3$@PEDOT electrode delivers a capacity of 128.5 mAh $g^{-1}$ at 0.1C which is about 96.6% of the theoretical capacity. At a high rate of 8C, it can still maintain a capacity of 108.6 mAh $g^{-1}$ for over 15 cycles with capacity decay rate of only 0.049% per cycle. The impressive electrochemical performance could be attributed to the coated PEDOT layer which can provide a fast electronic connection. Therefore, it can be make a conclusion that the core-shell $Li_3V_2(PO_4)_3$@PEDOT composite is a promising cathode material for next-generation lithium-ion batteries.



## 1. Introduction

Nowadays, rechargeable lithium-ion batteries are used in a wide range of applications from small portable electronic devices to hybrid electric vehicles (HEVs) or electric vehicles (EVs) [1,2]. Since the energy density of lithium-ion batteries is mainly determined by the intercalation compound cathodes, the cathode materials with high theoretical capacity, high operating voltage and low cost are widely investigated. Among currently studied cathodes for lithium-ion batteries, NASICON-type monoclinic $Li_3V_2(PO_4)_3$ electrode has become one of the most promising materials due to its high theoretical capacity, good safety and low cost [3–5]. It can completely extract three Li-ions when charged to a higher voltage of 4.8 V, which leads to a theoretical capacity of 197 mAh $g^{-1}$ [6,7]. Moreover, $Li_3V_2(PO_4)_3$ also exhibits a high operating voltage plateau (ca. 4.0 V), resulting in high energy density. Unfortunately, the low intrinsic electronic conductivity (ca. $2.4 \times 10^{-7}$ S $cm^{-1}$) and low Li-ion diffusion coefficient ($10^{-10}$–$10^{-9}$ $cm^2$ $s^{-1}$) of the pure $Li_3V_2(PO_4)_3$ electrode lead to a poor high rate performance, which thus limit its practical application [8].

Up to now, there have been several approaches to overcome the issues listed above. One effective way is to improve the intrinsic low conductivity by doping an appropriate amount of other alien ions (such as $Mg^{2+}$ [9], $Fe^{3+}$ [10], $Nd^{3+}$ [11], $Na^{+}$ [12], etc.) which can form a continuous conductive path in the electrode. Surface coating is another feasible way to enhance the battery performance by virtue of modifying the surface chemistry or providing protection layers to minimize the direct contact between the active material and electrolyte [13–15]. Among them, coating conductive carbon [16–21] can overcome the low electron conductivity of $Li_3V_2(PO_4)_3$ electrode, but the irregular coating may lead to poor connectivity of the particles and hence capacity loss. What's more, the Li-ion diffusion rate and the amount of lithium extracted from $Li_3V_2(PO_4)_3$ can be manipulated by synthesizing nanometer grain sizes [19], and thus the electrode material with nanometer sized particles is an ideal morphology to effectively improve the rate performance. Although these methods help to improve the battery performance of $Li_3V_2(PO_4)_3$, it still remains a challenge to realize its practical application for energy storage.

Recently, conducting polymers, such as polypyrrole (PPy) [22–24], polythiophene (PT) [25], polyaniline (PANI) [26,27], poly(3,4-ethylenedioxythiophene) (PEDOT) [28–31] have been used as coating agents for electrode surfaces in terms of improving the electronic conductivity and mechanical flexibility. Composite electrode materials with PEDOT are especially attractive in

* Corresponding author.
*E-mail address:* hyyan1979@163.com (H. Yan).

http://dx.doi.org/10.1016/j.apsusc.2016.09.156
0169-4332/

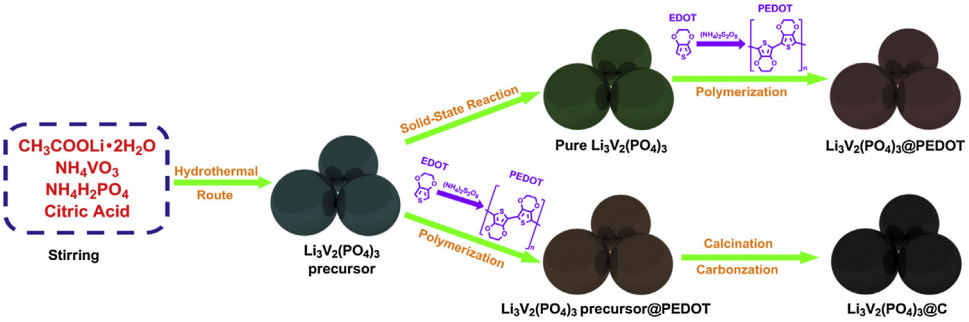


**Fig. 1.** Schematic illustration for the preparation of pure $Li_3V_2(PO_4)_3$, $Li_3V_2(PO_4)_3$@C and $Li_3V_2(PO_4)_3$@PEDOT samples.

terms of high electronic conductivity, contribution to the electrode capacity and the ability to improve Li-ion transport [32]. For example, Zhang et al. fabricated $Li_4Ti_5O_{12}$ modified with PEDOT via a facile method to enhance the rate performance [31]. Previously, Kang et al. reported that the battery performances of $Li_3V_2(PO_4)_3$ can be significantly improved by coating it with the conducting polymer PEDOT under mild processing conditions at low temperature without any conductive carbon, and the coating by means of oxidant-free polymerization led to an exceptionally high power capability with outstanding cycle stability [28]. Nevertheless, the $Li_3V_2(PO_4)_3$ should be partially delithiated during the synthesis process to oxidize the vanadium ions on the surface of the particles and it is difficult to control the composition of $Li_{3-x}V_2(PO_4)_3$. Thus, a facile and an effective strategy to synthesize PEDOT coated $Li_3V_2(PO_4)_3$ cathode should be developed toward superior rate capability and cycle performance.

In this study, the core-shell $Li_3V_2(PO_4)_3$@PEDOT composite is synthesized through a hydrothermal method followed by a chemical polymerization in the presence of oxidant. The structure, morphology and electrochemical performance of $Li_3V_2(PO_4)_3$@PEDOT electrode are investigated and compared with that of $Li_3V_2(PO_4)_3$ and $Li_3V_2(PO_4)_3$@C samples. Benefiting from the PEDOT coating layer with enhanced electronic conductivity, the $Li_3V_2(PO_4)_3$@PEDOT exhibits superior rate capability and cycling performance when used as cathode material for lithium-ion batteries.

## 2. Experimental

### 2.1. Materials synthesis

The pure $Li_3V_2(PO_4)_3$ sample was prepared by the previously reported hydrothermal method with minor modifications [33], as shown in Fig. 1. In a typical procedure, the stoichiometric amounts of $CH_3COOLi{\cdot}2H_2O$, $NH_4VO_3$ and $NH_4H_2PO_4$ were added to the distilled water and magnetically stirred at room temperature. Citric acid was then added to the above solution. The mixture was stirred for 2 h before being transferred into a 100 mL Teflon-lined autoclave. The autoclave was sealed, kept at 180 °C for 36 h and then cooled to room temperature naturally. The mixtures were heated gently with continuous stirring to remove the excess water at 80 °C. After drying at 100 °C overnight in an oven, the gel was ground, preheated at 350 °C for 4 h and finally calcined at 750 °C for 6 h under a flow of $N_2$ to obtain the pure $Li_3V_2(PO_4)_3$ product.

The conducting polymer PEDOT coated $Li_3V_2(PO_4)_3$ sample ($Li_3V_2(PO_4)_3$@PEDOT) was synthesized by a facile soft chemistry route as presented in Fig. 1. Firstly, the EDOT was added to the 0.1 M HCl solution with continuous stirring for 2 h. Then, the obtained pure $Li_3V_2(PO_4)_3$ and ammonium persulfate ($(NH_4)_2S_2O_8$) were added respectively and stirred for 12 h. During the synthesis procedure, the PEDOT layer was prepared through the oxidative polymerization of EDOT using the $(NH_4)_2S_2O_8$ as oxidation agent. Compared to the procedure of $Li_3V_2(PO_4)_3$/PEDOT reported by Kang [28], this approach does not involve the formation of chemical delithiation process. Finally, the powder was washed several times with distilled water and ethanol, and dried at 80 °C overnight to obtain the $Li_3V_2(PO_4)_3$@PEDOT composite. For comparison purposes, the carbon coated $Li_3V_2(PO_4)_3$ sample ($Li_3V_2(PO_4)_3$@C) sample was also prepared in a similar method using PEDOT as the carbon source. As illustrated in Fig. 1, the $Li_3V_2(PO_4)_3$ precursor@PEDOT was firstly prepared and then sintered at 600 °C for 3 h in an $N_2$ atmosphere to obtain the $Li_3V_2(PO_4)_3$@C product.

### 2.2. Material characterization

The crystal structures of pure $Li_3V_2(PO_4)_3$, $Li_3V_2(PO_4)_3$@C and $Li_3V_2(PO_4)_3$@PEDOT samples were investigated by X-ray diffraction patterns (XRD, Phillips, PW1700) equipped with Cu Kα radiation (λ = 0.15406 nm). The particle size distributions and particulate morphologies of the materials were observed using scanning electron microscopy (SEM, JEOL JSM-6390) and transmission electron microscopy (TEM, JEOL JEM-200CX). The microstructure property of $Li_3V_2(PO_4)_3$@PEDOT sample was carried out by scanning transmission electron microscopy-energy dispersive X-ray spectroscopy (STEM-EDS, JEOL JEM-200CX). The electronic conductivities of all the as-prepared samples were measured with an RTS-8 linear four-point probe measurement system.

### 2.3. Electrochemical test

Electrochemical characterization of the electrodes was performed by galvanostatic cycling in CR2025-type coin cells that were assembled in an argon-filled glove box. The working electrodes were fabricated by mixing the active material (86 wt.%), carbon black (7 wt.%) and polyvinylidene fluoride (PVDF, 7 wt.%) dissolved in *N*-methyl pyrrolidinone (NMP) and uniformly pasting the mixture on an Al current collector. Then, the electrodes were dried under vacuum at 100 °C for 12 h and cut into disks with a diameter of 14 mm. The average mass loading of active material was around 2.4 mg $cm^{-2}$. The coin cells were assembled with the cathodes thus fabricated, metallic lithium anode, Celgard 2400 film separator and 1 M $LiPF_6$ in 1:1 ethylene carbonate/dimethyl carbonate electrolyte. The charge/discharge cycle tests were performed at different current densities between 3.0 and 4.3 V (vs. $Li/Li^+$) using a land CT2001 tester (Wuhan, China), and the capacities were calculated based on the $Li_3V_2(PO_4)_3$ material. Cyclic voltammetry (CV) and electrochemical impedance spectra (EIS) tests were carried out on a Zahner Zennium electrochemical workstation. CV test was performed at a scan rate of 0.2 mV $s^{-1}$ on the potential interval 3.0–4.3 V (vs. $Li/Li^+$), and the EIS was tested with an ac amplitude of 5 mV in the frequency range from 0.01 Hz to 100 kHz. All the measurements were carried out at room temperature.

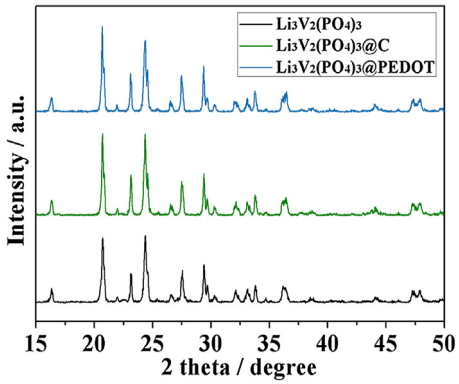


**Fig. 2.** XRD patterns of $Li_3V_2(PO_4)_3$, $Li_3V_2(PO_4)_3$@C and $Li_3V_2(PO_4)_3$@PEDOT powders.

## 3. Results and discussion

The phase purity and crystal structure of the as-prepared $Li_3V_2(PO_4)_3$, $Li_3V_2(PO_4)_3$@C and $Li_3V_2(PO_4)_3$@PEDOT samples were investigated by XRD, as shown in Fig. 2. Based on the XRD results, it can be noted that all the diffraction peaks of the three samples can be indexed as monoclinic $Li_3V_2(PO_4)_3$ phase with a space group $P2_1/n$ (JCPDS card No. 43-0526), which are consistent with the previous reports [16–21,29]. For the $Li_3V_2(PO_4)_3$@C sample, there is no diffraction peak of carbon, revealing the residual carbon is amorphous. Importantly, no contamination or secondary phases introduced by PEDOT coating are detected in the XRD patterns of $Li_3V_2(PO_4)_3$@PEDOT composite. What's more, the lattice parameters of $Li_3V_2(PO_4)_3$@PEDOT are a = 8.5875 Å, b = 8.6113 Å, c = 12.0259 Å and β = 90.572°, which are in good agreement with the reported literature [29].

Fig. 3 illustrates the SEM, TEM and HRTEM images of $Li_3V_2(PO_4)_3$, $Li_3V_2(PO_4)_3$@C and $Li_3V_2(PO_4)_3$@PEDOT samples. It can be found that the pure $Li_3V_2(PO_4)_3$ and $Li_3V_2(PO_4)_3$@C show a nonuniform morphology, comprising of different sized particles range from 50 to 200 nm (see Fig. 3a and b). After intruding the conducting PEDOT coating (see Fig. 3c), the particle size is about 140 nm on an average and the surface is almost the same as the pure $Li_3V_2(PO_4)_3$ and $Li_3V_2(PO_4)_3$@C which is similar to the PEDOT coated $Li_4Ti_5O_{12}$ electrode [31]. Thus, the morphologies of the as-prepared samples were further characterized by TEM and HRTEM. The TEM and HRTEM images show that the surface of the pure $Li_3V_2(PO_4)_3$ sample (see Fig. 3d and g) is very smooth, whereas the surface of $Li_3V_2(PO_4)_3$@C (see Fig. 3e and h) is coated with a thin amorphous layer (8 nm) which should be the carbon coating. Fig. 3f and i gives the TEM and HRTEM images of $Li_3V_2(PO_4)_3$@PEDOT

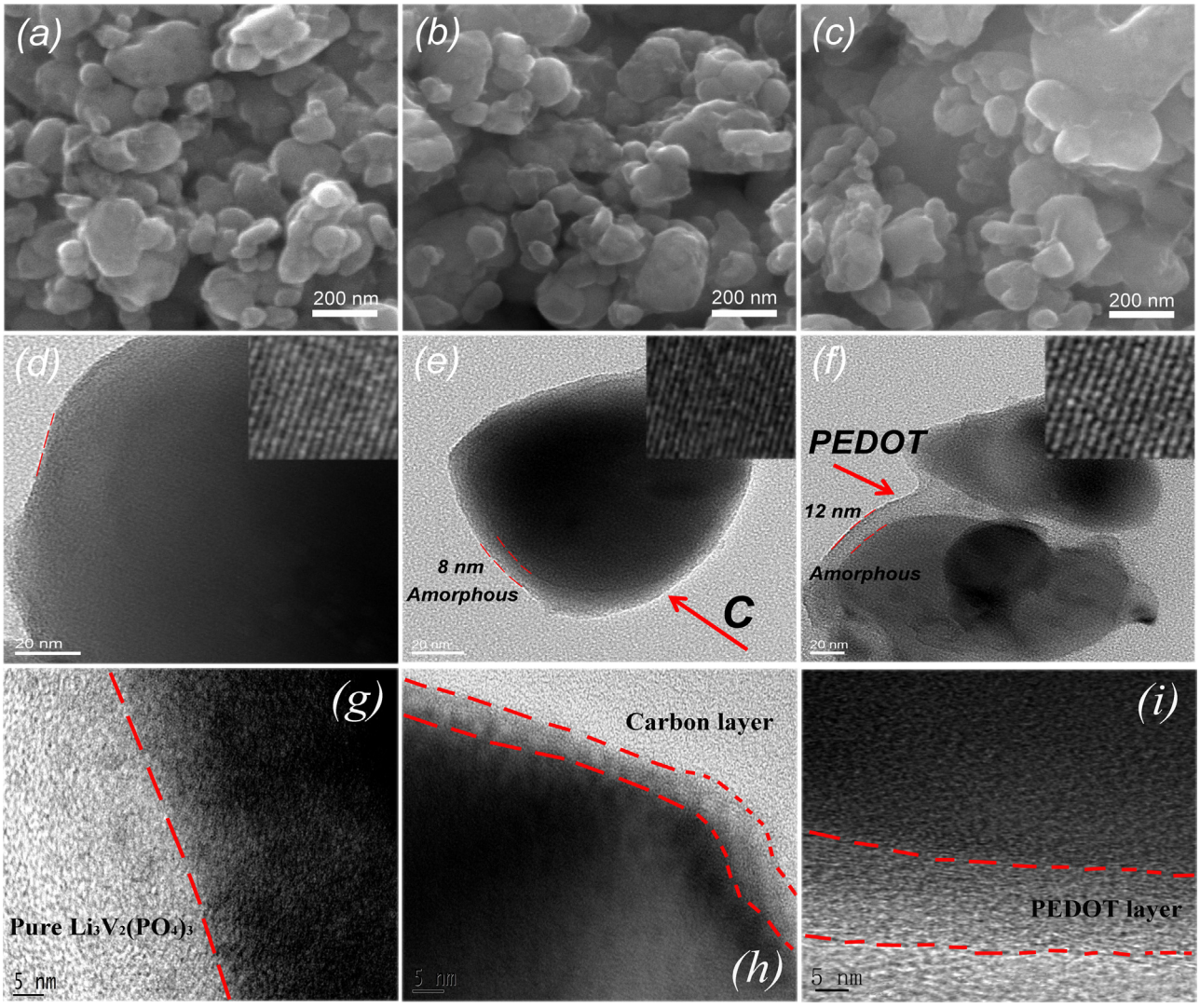


**Fig. 3.** SEM, TEM and HRTEM images of (a, d and g) pure $Li_3V_2(PO_4)_3$, (b, e and h) $Li_3V_2(PO_4)_3$@C and (c, f and i) $Li_3V_2(PO_4)_3$@PEDOT samples.

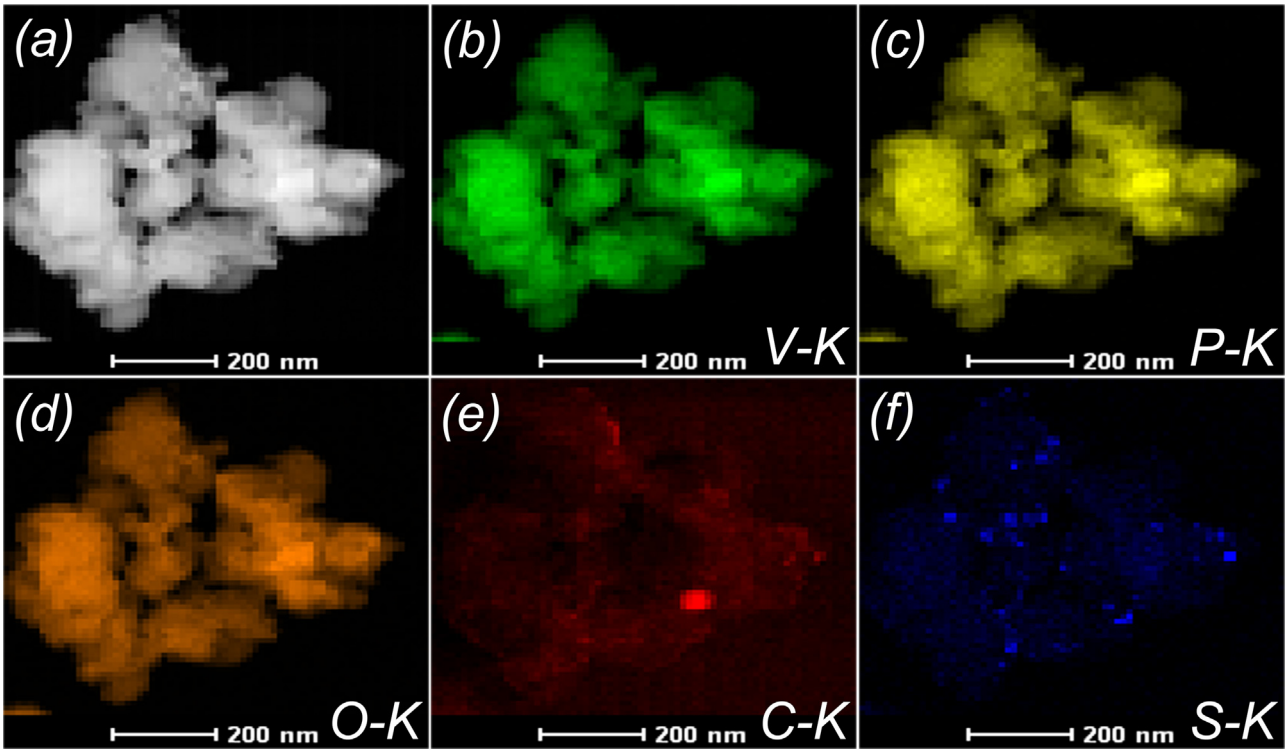


**Fig. 4.** (a) STEM image for the $Li_3V_2(PO_4)_3$@PEDOT particles, and the related EDS mapping images of (b) V, (c) P, (d) O, (e) C and (f) S elements.

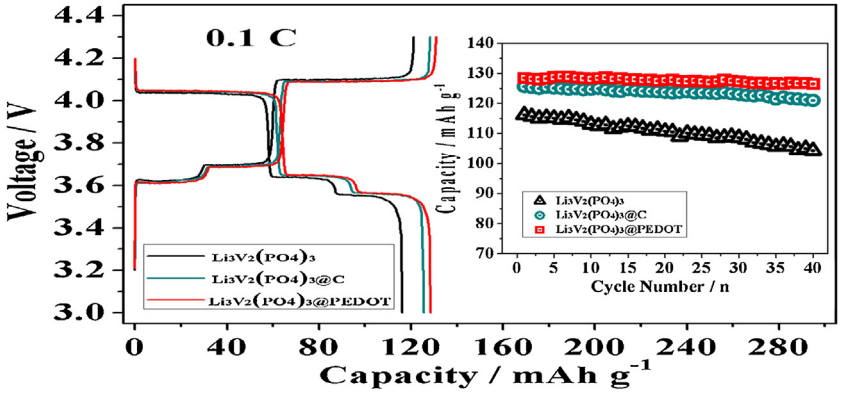


**Fig. 5.** Initial charge/discharge profiles and cycle performances (shown in the inset) of the as-prepared $Li_3V_2(PO_4)_3$, $Li_3V_2(PO_4)_3$@C and $Li_3V_2(PO_4)_3$@PEDOT materials at a low rate of 0.1C between 3.0 and 4.3 V.

composite, from which it can be seen that the $Li_3V_2(PO_4)_3$ nanoparticles have a diameter of 50–140 nm and the conducting PEDOT (12 nm) are homogeneously attached to the surface of $Li_3V_2(PO_4)_3$ particles. The HRTEM images (inset in Fig. 3d–f) reveal the high crystallization character of all the samples. In this study, it should be pointed out that the weight percentage of carbon and PEDOT in $Li_3V_2(PO_4)_3$@C and $Li_3V_2(PO_4)_3$@PEDOT samples are about 7.8 wt.% and 9.5 wt.%, respectively, according to the thermogravimetric analysis (TGA). To the best of our knowledge, the mass loading of PEDOT in $Li_3V_2(PO_4)_3$/conducting polymer [28] is about 13 wt.%, which is higher than that of $Li_3V_2(PO_4)_3$@PEDOT composite in this paper. In addition, the carbon contents of $Li_3V_2(PO_4)_3$/C-M-NWs (9.7 wt.%), $Li_3V_2(PO_4)_3$@CMK-3 (10.1 wt.%) and N-$Li_3V_2(PO_4)_3$@C (15.1 wt.%) samples reported in the previous literatures [16,17,19] are also higher than that of the as-fabricated $Li_3V_2(PO_4)_3$@C in this study.

To further prove the existence of PEDOT, the STEM and EDS dot mapping tests were carried out. The analysis of element distribution mapping by EDS (see Fig. 4b–d) displays rather uniform distribution of V, P and O elements in $Li_3V_2(PO_4)_3$@PEDOT composite. As illustrated in Fig. 4e and f, it can be noted that both C and S elements are also uniformly distributed, giving unequivocal evidence to the presence of PEDOT coating on the surface of $Li_3V_2(PO_4)_3$ particles. The above results are consistent well with the previous paper [29].

Fig. 5 shows the initial charge/discharge profiles and cycle performances of the as-prepared $Li_3V_2(PO_4)_3$, $Li_3V_2(PO_4)_3$@C and $Li_3V_2(PO_4)_3$@PEDOT electrodes at a low rate of 0.1C (1C = 133 mAh $g^{-1}$) between 3.0 and 4.3 V. Obviously, there are three flat plateaus on each branch originating from reversible phase transformation of $Li_xV_2(PO_4)_3$ (x = 2.5, 2.0, 1.0) occurred during the Li-ion insertion/extraction [34]. At 0.1C, the initial discharge capacities of $Li_3V_2(PO_4)_3$ and $Li_3V_2(PO_4)_3$@C are 116.2 and 125.6 mAh $g^{-1}$, respectively. However, the $Li_3V_2(PO_4)_3$@PEDOT sample delivers a discharge capacity of 128.5 mAh $g^{-1}$, which is close to its theoretical capacity of 133 mAh $g^{-1}$. The inset in Fig. 5 gives the cycle

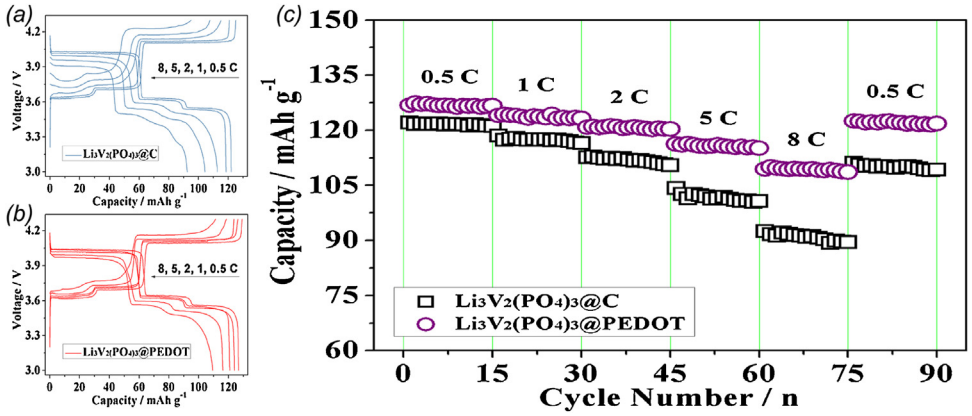


**Fig. 6.** Rate performance of $Li_3V_2(PO_4)_3$@C and $Li_3V_2(PO_4)_3$@PEDOT materials at various current rates increased from 0.5C to 8C between 3.0 and 4.3 V.

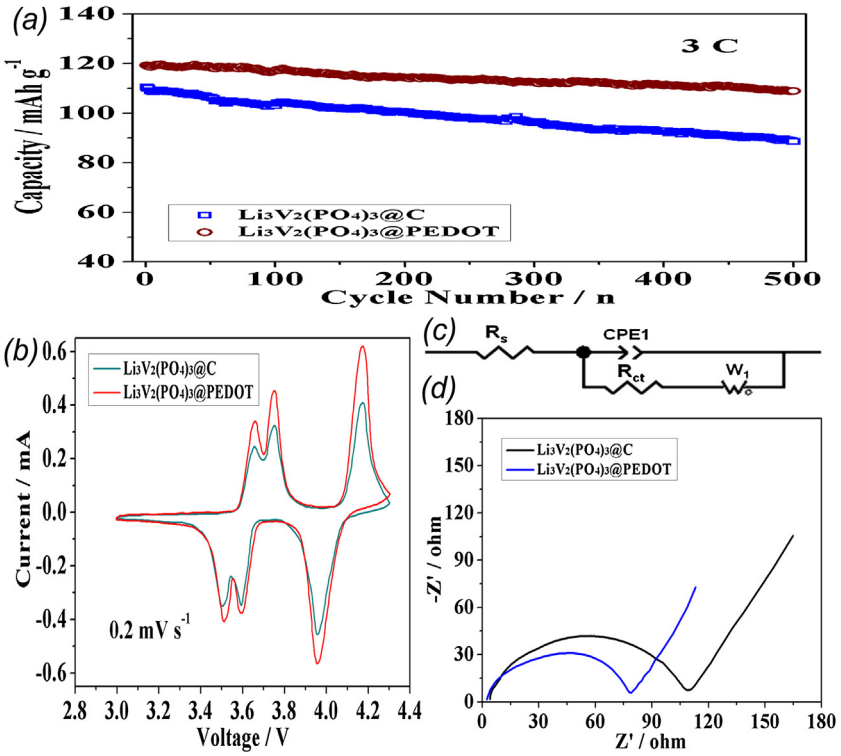


**Fig. 7.** (a) Comparison of the long-cycle ability of $Li_3V_2(PO_4)_3$@C and $Li_3V_2(PO_4)_3$@PEDOT at 3C for 500 cycles; (b) CV curves of $Li_3V_2(PO_4)_3$@C and $Li_3V_2(PO_4)_3$@PEDOT cathode materials at a scan rate of 0.2 mV $s^{-1}$ in the potential range of 3.0 to 4.3 V versus $Li/Li^+$; (c) The equivalent circuit used to fit the impedance data; (d) Nyquist plots of the two electrodes with an ac amplitude of 5 mV in the frequency range from 0.01 Hz to 100 kHz.

performances at 0.1C for 40 cycles. Clearly, the discharge capacity of the pure $Li_3V_2(PO_4)_3$ drops rapidly during the cycling process, owing the poor electronic conductivity. For the $Li_3V_2(PO_4)_3$@C electrode, it shows a discharge capacity of 121 mAh $g^{-1}$ after 40 cycles, with a capacity retention of 96.3%. Just as expected, the $Li_3V_2(PO_4)_3$@PEDOT exhibits a better cycle performance than $Li_3V_2(PO_4)_3$@C, similar to the PEDOT modified electrodes [29,31]. This is mainly attributed to the existence of conducting PEDOT layer which can greatly enhance the electronic conductivity of the electrode and thus accelerate the electron transport.

The rate performance of $Li_3V_2(PO_4)_3$@C and $Li_3V_2(PO_4)_3$@PEDOT materials at various current rates increased from 0.5C to 8C between 3.0 and 4.3 V are also evaluated. As illustrated in Fig. 6a, with the increase of current density, the discharge plateau voltages of $Li_3V_2(PO_4)_3$@C decrease quickly and the electrochemical plateaus become undistinguishable, due to the increase of cell polarization at high current rates [35]. It delivers discharge capacities of 122.1, 118.5, 112.6, 104.3 and 92.5 mAh $g^{-1}$ at 0.5C, 1C, 2C, 5C and 8C, respectively. For the $Li_3V_2(PO_4)_3$@PEDOT composite (Fig. 6b), the electrode presents a high discharge capacity of 126.8 mAh $g^{-1}$ at 0.5C; even at high rate of 8C, it can still deliver a discharge capacity of 109.4 mAh $g^{-1}$. This superior rate performance is also better than that of the carbon coated $Li_3V_2(PO_4)_3$ electrodes [34,36]. Noticeably, a more stable potential plateau during the charge/discharge process for the $Li_3V_2(PO_4)_3$@PEDOT electrode reveals a more alleviated polarization. The cycle performances of the two electrodes at various current rates are shown in Fig. 6c. At low current rates, both electrodes show stable discharge capacities. However, when the rate is higher than 2C, the difference in the rate performance becomes obvious. It is clear that, when the current rate was reduced back to 0.5C, the discharge capacities of $Li_3V_2(PO_4)_3$@PEDOT

electrode can almost recover its initial capacity value, whereas the $Li_3V_2(PO_4)_3$@C returns to only about 91% of its initial capacity.

To further study the battery performances of $Li_3V_2(PO_4)_3$@C and $Li_3V_2(PO_4)_3$@PEDOT electrodes, the long-cycle ability at 3C for 500 cycles was tested. As shown in Fig. 7a, compared with $Li_3V_2(PO_4)_3$@C, the $Li_3V_2(PO_4)_3$@PEDOT presents higher cycling capacity (108.9 mAh $g^{-1}$ after 500 cycles) and capacity retention (91.3% after 500 cycles), corresponding to low capacity decay ratio of 0.0174% per cycle. The excellent cycle stability is because the existence of PEDOT can accelerate the electron transport during the cycling process. Fig. 7b illustrates the CV curves of the two electrodes at a scan rate of 0.2 mV $s^{-1}$ in the voltage range of 3.0–4.3 V. It can be seen that both $Li_3V_2(PO_4)_3$@C and $Li_3V_2(PO_4)_3$@PEDOT present three couples of oxidation and reduction peaks between 3.0 and 4.3 V. Such peaks are associated with two Li-ions extraction/insertion out/into of the $Li_3V_2(PO_4)_3$ lattice based on the $V^{3+}/V^{4+}$ redox couple [37]. The series of reversible phase transitions can be written as the following equations [19,38].

(1) $Li_3V_2(PO_4)_3 \leftrightarrow Li_{2.5}V_2(PO_4)_3 + 0.5Li^+ + 0.5e^-$

(2) $Li_{2.5}V_2(PO_4)_3 \leftrightarrow Li_2V_2(PO_4)_3 + 0.5Li^+ + 0.5e^-$

(3) $Li_2V_2(PO_4)_3 \leftrightarrow LiV_2(PO_4)_3 + Li^+ + e^-$

Compared with the $Li_3V_2(PO_4)_3$@C electrode, the peaks of $Li_3V_2(PO_4)_3$@PEDOT are sharper and have a higher intensity. Besides, the potential difference between the anodic peaks and the corresponding cathodic peaks of $Li_3V_2(PO_4)_3$@PEDOT electrode is also smaller than that of $Li_3V_2(PO_4)_3$@C, revealing an alleviated polarization and easier extraction/insertion of Li-ion in the $Li_3V_2(PO_4)_3$ lattice.

To better understand the electrochical performances of the electrodes, EIS measurement was performed. The equivalent circuit presented in Fig. 7c is used to fit the impedance data. Fig. 7d shows the Nyquist plots of $Li_3V_2(PO_4)_3$@C and $Li_3V_2(PO_4)_3$@PEDOT which exhibit a semicircle in the high-frequency region and a straight line in the low frequency region. The small intercept is related to the solution resistance ($R_s$), the depressed semicircle at medium frequency represents the charge-transfer resistance ($R_{ct}$) and the double-layer capacitance ($C_{dl}$), and the sloping line at low frequency is attributed to the Warburg impedance associated with the diffusion of Li-ion in the electrode ($Z_w$) [39]. Clearly, the charge-transfer resistance of $Li_3V_2(PO_4)_3$@PEDOT (78 Ω) is lower than that of the $Li_3V_2(PO_4)_3$@C electrode (109 Ω), which is likely because of the increase in electronic conductivity that results from the conducting PEDOT coating. Moreover, the electronic conductivities of all the samples were measured by the four-electrode method, and the conductivity of $Li_3V_2(PO_4)_3$@PEDOT reaches $9.5 \times 10^{-4}$ S $cm^{-1}$, as compared with that of the pure $Li_3V_2(PO_4)_3$ ($3.7 \times 10^{-5}$ S $cm^{-1}$) and $Li_3V_2(PO_4)_3$@C ($6.2 \times 10^{-4}$ S $cm^{-1}$), revealing that the PEDOT layer plays an important role in enhancing the electronic conductivity of $Li_3V_2(PO_4)_3$. Thus, the $Li_3V_2(PO_4)_3$@PEDOT composite exhibits superior rate capability and cycle stability when used as cathode material for lithium-ion batteries.

## 4. Conclusions

In summary, the conducting polymer PEDOT layer has been successfully coated on the surface of $Li_3V_2(PO_4)_3$ electrode through a facile chemical polymerization method. The structure and morphology of the as-synthesized core-shell $Li_3V_2(PO_4)_3$@PEDOT composite are investigated by the techniques of XRD, SEM, TEM and EDS. It is found that the thickness of the polymerized PEDOT layer covering on the $Li_3V_2(PO_4)_3$ nanoparticles is about 3–10 nm. The electrochemical measurements demonstrate that the reversible capacity, rate capability and cycling performance of $Li_3V_2(PO_4)_3$ cathode have been greatly improved by PEDOT coating, which could maintain a reversible capacity of 108.9 mAh $g^{-1}$ after 500 cycles at 3C.

The superior performance is ascribed to an enhanced electronic conductivity of the electrode emerging from the conductive nature of PEDOT, and it also reveal that this core-shell structured $Li_3V_2(PO_4)_3$@PEDOT has a promising application as cathode material for high energy lithium-ion batteries.

## Acknowledgments

This research was financially supported by the Shanxi Provincial Training Program of Innovation and Entrepreneurship for Undergraduates (grant No. 201510702045), and the National Natural Science Foundation of China (grant No. 21501139).

## References

[1] E. Karden, S. Ploumen, B. Fricke, T. Miller, K. Snyder, Energy storage devices for future hybrid electric vehicles, J. Power Sources 168 (2007) 2–11.
[2] H. Li, Z.X. Wang, L.Q. Chen, X.J. Huang, Research on advanced materials for Li-ion batteries, Adv. Mater. 21 (2009) 4593–4607.
[3] H. Huang, S.C. Yin, T. Kerr, N. Taylor, L.F. Nazar, Nanostructured composites: a high capacity fast rate $Li_3V_2(PO_4)_3$/carbon cathode for rechargeable lithium batteries, Adv. Mater. 14 (2002) 1525–1528.
[4] L.L. Zhang, X. Zhang, Y.M. Sun, W. Luo, X.L. Hu, X.J. Wu, Y.H. Huang, Improved electrochemical performance in $Li_3V_2(PO_4)_3$ promoted by niobium-incorporation batteries and energy storage, J. Electrochem. Soc. 158 (2011) A924–A929.
[5] D. Morgan, G. Ceder, M.Y. Saidi, J. Barker, J. Swoyer, G. Adamson, Experimental and computational study of the structure and electrochemical properties of monoclinic $Li_xM_2(PO_4)_3$ compounds, J. Power Sources 119-121 (2003) 755–759.
[6] J. Wang, J. Liu, G. Yang, X. Zhang, X. Yan, X. Pan, R. Wang, Electrochemical performance of $Li_3V_2(PO_4)_3$/C cathode material using a novel carbon source, Electrochim. Acta 54 (2009) 6451–6454.
[7] S.C. Yin, H. Grondey, P. Strobel, M. Anne, L.F. Nazar, Electrochemical property: structure relationships in monoclinic $Li_{3-y}V_2(PO_4)_3$, J. Am. Chem. Soc. 125 (2003) 10402–10411.
[8] L. Dimesso, C. Forster, W. Jaegermann, J.P. Khanderi, H. Tempel, A. Popp, J. Engstler, J.J. Schneider, A. Sarapulova, D. Mikhailova, L.A. Schmitt, S. Oswald, H. Ehrenberg, Development in nanostructured $LiMPO_4$ (M = Fe, Co Ni, Mn) composites based on three dimensional carbon architecture, Chem. Soc. Rev. 41 (2012) 5068–5080.
[9] J.S. Huang, L. Yang, K.Y. Liu, Y.F. Tang, Synthesis and characterization of $Li_3V_{(2-2x/3)}Mg_x(PO_4)_3$/C cathode material for lithium-ion batteries, J. Power Sources 195 (2010) 5013–5018.
[10] Y.H. Kee, N. Dimov, E. Kobayashi, A. Kitajou, S. Okada, Structural and electrochemical properties of Fe- and Al-doped $Li_3V_2(PO_4)_3$ for all-solid-state symmetric lithium ion batteries prepared by spray-drying-assisted carbothermal method, Solid State Ionics 272 (2015) 138–143.
[11] Y.L. Wang, L.H. Wang, Z.Z. Hou, W.X. Mao, Effects of Nd-doping on the structure and electrochemical properties of $Li_3V_2(PO_4)_3$/C synthesized using a microwave solid-state route, Solid State Ionics 261 (2014) 11–16.
[12] J.L. Mao, L.Y. Shao, P. Li, X.T. Lin, M. Shui, N.B. Long, J. Shu, Comparison of phase composition morphology and electrochemical property for $Li_{3-x}Na_xV_2(PO_4)_3$ (x = 0.5, 1.5 and 2.0) as lithium storage cathode materials, Electrochim. Acta 173 (2015) 96–104.
[13] Effects of $Al_2O_3$ and $AlF_3$ coating on the electrochemical performance of $Li_3V_2(PO_4)_3$/C cathode material in lithium ion batteries, Solid State Ionics 283 (2015) 131–136.
[14] D. Guan, J.A. Jeevarajan, Y. Wang, Enhanced cycleability of $LiMn_2O_4$ cathodes by atomic layer deposition of nanosized-thin $Al_2O_3$ coatings, Nanoscale 3 (2011) 1465–1469.
[15] C.Y. Lai, J.J. Wei, Z. Wang, Q.J. Xu, Y.F. Lu, H.X. Li, $Li_3V_2(PO_4)_3$/($SiO_2$ + C) composite with better stability and electrochemical properties for lithium-ion batteries, Solid State Ionics 272 (2015) 121–126.
[16] Q.L. Wei, Q.Y. An, D.D. Chen, L.Q. Mai, S.Y. Chen, Y.L. Zhao, K.M. Hercule, L. Xu, A. Minhas-Khan, Q.J. Zhang, One-pot synthesized bicontinuous hierarchical $Li_3V_2(PO_4)_3$/C mesoporous nanowires for high-rate and ultralong-life lithium-ion batteries, Nano Lett. 14 (2014) 1042–1048.
[17] S.L. Wang, Z.X. Zhang, Z.T. Jiang, A. Deb, L. Yang, S.I. Hirano, Mesoporous $Li_3V_2(PO_4)_3$@CMK-3 nanocomposite cathode material for lithium ion batteries, J. Power Sources 253 (2014) 294–299.
[18] R.Y. Zhang, X. Yang, Y. Gao, Y.M. Ju, H.L. Qiu, X. Meng, G. Chen, Y.J. Wei, In-situ preparation of $Li_3V_2(PO_4)_3$/C and carbon nanofibers hierarchical cathode by the chemical vapor deposition reaction, Electrochim. Acta 188 (2016) 254–261.
[19] W.C. Duan, Z. Hu, K. Zhang, F.Y. Cheng, Z.L. Tao, J. Chen, $Li_3V_2(PO_4)_3$@C core-shell nanocomposite as a superior cathode material for lithium-ion batteries, Nanoscale 5 (2013) 6485–6490.

[20] Y.Q. Qiao, X.L. Wang, Y.J. Mai, J.Y. Xiang, D. Zhang, C.D. Gu, J.P. Tu, Synthesis of plate-like $Li_3V_2(PO_4)_3$/C as a cathode material for Li-ion batteries, J. Power Sources 196 (2011) 8706–8709.
[21] Q.Z. Ou, Y. Tang, Y.J. Zhong, X.D. Guo, B.H. Zhong, H. Liu, M.Z. Chen, Submicrometer porous $Li_3V_2(PO_4)_3$/C composites with high rate electrochemical performance prepared by sol-gel combustion method, Electrochim. Acta 137 (2014) 489–496.
[22] Y. Liu, B.H. Zhang, S.Y. Xiao, L.L. Liu, Z.B. Wen, Y.P. Wu, A nanocomposite of $MoO_3$ coated with PPy as an anode material for aqueous sodium rechargeable batteries with excellent electrochemical performance, Electrochim. Acta 116 (2014) 512–517.
[23] X.W. Gao, Y.F. Deng, D. Wexler, G.H. Chen, S.L. Chou, H.K. Liu, Z.C. Shi, J.Z. Wang, Improving the electrochemical performance of the $LiNi_{0.5}Mn_{1.5}O_4$ spinel by polypyrrole coating as a cathode material for the lithium-ion battery, J. Mater. Chem. A 3 (2015) 404–411.
[24] J.K. Kim, J. Manuel, M.H. Lee, J. Scheers, D.H. Lim, P. Johansson, J.H. Ahn, A. Matic, P. Jacobsson, Towards flexible secondary lithium batteries: polypyrrole-$LiFePO_4$ thin electrodes with polymer electrolytes, J. Mater. Chem. 22 (2012) 15045–15049.
[25] E. Tahmasebi, Y. Yamini, M. Moradi, A. Esrafili, Polythiophene-coated $Fe_3O_4$ superparamagnetic nanocomposite: synthesis and application as a new sorbent for solid-phase extraction, Anal. Chim. Acta 770 (2013) 68–74.
[26] Z.Y. Hai, L.B. Gao, Q. Zhang, H.Y. Xu, D.F. Cui, Z.X. Zhang, D. Tsoukalas, J. Tang, S.B. Yan, C.Y. Xue, Facile synthesis of core-shell structured PANI-$Co_3O_4$ nanocomposites with superior electrochemical performance in supercapacitors, Appl. Surf. Sci. 361 (2016) 57–62.
[27] Y.L. An, P. Wei, M.Q. Fan, D. Chen, H.C. Chen, Q.J. Ju, G.L. Tian, K.Y. Shu, Dual-shell hollow polyaniline/sulfur-core/polyaniline composites improving the capacity and cycle performance of lithium-sulfur batteries, Appl. Surf. Sci. 375 (2016) 215–222.
[28] J. Kim, J.K. Yoo, Y.S. Jung, K. Kang, $Li_3V_2(PO_4)_3$/conducting polymer as a high power 4 V-class lithium battery electrode, Adv. Energy Mater. 3 (2013) 1004–1007.
[29] X.L. Zhao, Y.J. Mai, H. Luo, D.P. Tang, B.H. Lee, C.G. Huang, L.Z. Zhang, 4Nano-$MoS_2$/poly (3,4-ethylenedioxythiophene): Poly(styrenesulfonate) composite prepared by a facial dip-coating process for Li-ion battery anode, Appl. Surf. Sci. 288 (2014) 736–741.
[30] T.M. Higgins, S.H. Park, P.J. King, C.F. Zhang, N. McEvoy, N.C. Berner, D. Daly, A. Shmeliov, U. Khan, G. Duesberg, V. Nicolosi, J.N. Coleman, A commercial conducting polymer as both binder and conductive additive for silicon nanoparticle-based lithium-ion battery negative electrodes, ACS Nano 10 (2016) 3702–3713.
[31] X.Y. Wang, L.F. Shen, H.S. Li, J. Wang, H. Dou, X.G. Zhang, PEDOT coated $Li_4Ti_5O_{12}$ nanorods: soft chemistry approach synthesis and their lithium storage properties, Electrochim. Acta 129 (2014) 283–289.
[32] K. Abe, Y. Ushigoe, H. Yoshitake, M. Yoshio, Functional electrolytes: novel type additives for cathode materials providing high cycleability performance, J. Power Sources 153 (2006) 328–335.
[33] C.W. Sun, S. Rajasekhara, Y.Z. Dong, J.B. Goodenough, Hydrothermal synthesis and electrochemical properties of $Li_3V_2(PO_4)_3$/C-based composites for lithium-ion batteries, ACS Appl. Mater. Interfaces 3 (2011) 3772–3776.
[34] H. Chen, Z.K. Wang, G.D. Li, F.F. Guo, M.H. Fan, X.Y. Wu, X.C. Cao, Enhanced electrochemical performance of $Li_3V_2(PO_4)_3$ microspheres assembled with nanoparticles embedded in a carbon matrix, RSC Adv. 5 (2015) 31410–31414.
[35] D.L. Li, M. Tian, R. Xie, Q. Li, X.Y. Fan, P. Zhao, S.L. Ma, Y.X. Shi, H.T.H. Yong, Three-dimensionally ordered macroporous $Li_3V_2(PO_4)_3$/C nanocomposite cathode material for high-capacity and high-rate Li-ion batteries, Nanoscale 6 (2014) 3302–3308.
[36] C.L. Zhang, H.S. Li, N. Ping, G. Pang, G.Y. Xu, X.G. Zhang, Facile synthesis of nitrogen-doped carbon derived from polydopamine-coated $Li_3V_2(PO_4)_3$ as cathode material for lithium-ion batteries, RSC Adv. 4 (2014) 38791–38796.
[37] M.Y. Saydi, J. Barker, H. Huang, J.L. Swoyer, G. Adamson, Performance characteristics of lithium vanadium phosphate as a cathode material for lithium-ion batteries, J. Power Sources 119–121 (2003) 266–272.
[38] C. Wang, H.M. Liu, W.S. Yang, An integrated core-shell structured $Li_3V_2(PO_4)_3$@C cathode material of LIBs prepared by a momentary freeze-drying method, J. Mater. Chem. 22 (2012) 5281–5285.
[39] M.V. Reddy, G.V. Subba Rao, B.V.R. Chowdari, Preparation and characterization of $LiNi_{0.5}Co_{0.5}O_2$ and $LiNi_{0.5}Co_{0.4}Al_{0.1}O_2$ by molten salt synthesis for Li ion batteries, J. Phys. Chem. C 111 (2007) 11712–11720.